Applying a biodeposition layer to increase the bond of a repair mortar on a mortar substrate

D. Snoeck [a], J. Wang [a,b], D.P. Bentz [c], N. De Belie [a,*]

[a] Magnel Laboratory for Concrete Research, Department of Structural Engineering, Faculty of Engineering and Architecture, Ghent University, Tech Lane Ghent Science Park, Campus A, Technologiepark Zwijnaarde 904, B-9052 Gent, Belgium

[b] Center for Microbial Ecology and Technology, Ghent University, Coupure Links 653, 9000 Ghent, Belgium

[c] Engineering Laboratory, National Institute of Standards and Technology, 100 Bureau Drive, Stop 8615, Gaithersburg, MD 20899, USA

* Corresponding author. Fax: 0032(0)92645845, Tel: 0032(0)92645522, e-mail: nele.debelie@UGent.be

Abstract

One of the major concerns in infrastructure repair is a sufficient bond between the substrate and the repair material, especially for the long-term performance and durability of the repaired structure. In this study, the bond of the repair material on the mortar substrate is promoted via the biodeposition of a calcium carbonate layer by a ureolytic bacterium. X-ray diffraction and scanning electron microscopy were used to examine the interfaces between the repair material and the substrate, as well as the polymorph of the deposited calcium carbonate.

The approximately 50 µm thick biodeposition film on the mortar surface mostly consisted of calcite and vaterite. Both the repair material and the substrate tended to show a good adherence to that layer. The bond, as assessed by slant shear specimen testing, was improved by the presence of the biodeposition layer. A further increase was found when engineering the substrate surface using a structured pattern layer of biodeposition.

Keywords:

B. EDX; B. X-Ray Diffraction; C. Bond strength; E. Mortar; Bacteria; Biodeposition

1. Introduction

Concrete is one of the most widely used construction materials on Earth. It is an ideal material to resist compressive forces, but when sufficient tensile forces are present, concrete may crack. And, without repair of the cracks, the durability can be critically compromised. One can decide to use a self-healing concrete during the design phase of construction [1-3], but repair of existing concrete structures will still often be needed. This manual repair should be made with care and precautions should be taken to assure that the repair is long-lasting, durable and efficient. If the bond between repair product and concrete substrate is not sufficient, delamination or spalling may occur. Therefore, one needs to make sure that the surface treatment of the substrate is properly executed. A striking statistic is that, 20%, 55% and 90% of the repairs of concrete structures are unsatisfactory after only 5, 10 and 25 years, respectively [4]. For patch repair, 30% of the failures are due to cracking, 25% due to debonding, 25% due to corrosion issues and 20% due to other failure mechanisms [4]. Debonding thus is a major factor in the overall failure of repair works [5].

One way of improving the bond between a concrete substrate and a repair material is by introducing a primer on the substrate. For example, incorporating fly ash into a primer between both materials or using neat cement paste, expansive paste, cement mortar or a water-dispersible epoxy resin as a primer are existing solutions [6]. A silane coupling agent can be applied as well [7]. But, the bond of the coupling agent itself should also be good and the practitioner would thus benefit from a solution where the bond is not a possible issue. Also, proper surface preparation, as characterized by cleanliness, roughness, and saturation level, is of major importance [8-10].

Another way of increasing and engineering the bond between the repair material and the concrete substrate could be the use of a biodeposition treatment, which is based on bacterially induced $CaCO_3$ precipitation in/on the substrate. One of the first patented applications on biodeposition was the protection of ornamental stone by a microbially deposited carbonate layer [11, 12]. The formed bacterial $CaCO_3$ layer works as an extra barrier to resist degradation and/or as a consolidant to cement the loose particles, and hence the surface properties of historical materials can be greatly enhanced in the aspects of a decrease of water permeability, an increase of freeze-thaw resistance, and an improvement of surface strength, etc. [13-15].This biodeposition technique has also been applied on cementitious materials resulting in an increased resistance of mortar specimens towards chloride penetration, freeze/thawing and carbonation [11, 15-17]. It should merely be considered as a coating system as carbonate precipitation is mainly a surface-controlled phenomenon due to the limited penetration of bacteria into the microporous cementitious matrix. Thin-section analysis revealed that the thickness of the bacterial layer was typically within the range of 10 µm to 40 µm; in which larger crystals up to 110 µm could be found [11]. This layer may be a promising route to engineer the substrate surface for optimal bond strength characteristics.

The bond between the concrete or mortar substrate and the repair material usually represents the weak link in the repaired structure if no special action is undertaken. Several tests are currently available to measure the bond of the repair material to the substrate. The main tests under tensile stress are pull-off tests, direct tension tests, and splitting tensile tests. Direct shear methods are also used. A combination of both shear and compression can be used as well. An example is the slant shear test where two identical halves bonded at an angle of 30° are tested under axial compression. Depending on the method, different quantitative values may be obtained for the bond strength [8, 18]. The slant shear test has become one of the most-widely accepted tests.

In this paper, the bond strength was assessed by slant shear testing. Specimens with and without a biodeposited layer were studied and the crystal composition and morphology were examined. Different partial pattern-type biodeposition layers were studied to further increase the bond strength between a mortar substrate and a repair material. The formed biodeposition products were studied by means of X-ray diffraction, scanning electron microscopy and thin section analysis.

2. Materials and methods

2.1 Mortar specimens

The standard followed to prepare the mortar substrates was ASTM C882/C882M-13 on ‘Bond strength of epoxy-resin systems used with concrete by slant shear’. Three portland-cement mortar cylinders with a standard mixture composition as described in the Standard EN 196-1 were cast (510 kg/m^3 CEM I 52.5 N, 1530 kg/m^3 silica sand 0/2, and 255 kg/m^3 water) per series. The specimens’ diameter and height were 75 mm and 150 mm, respectively, and each had a diagonally cast bonding area at a 30° angle from the vertical, as per the ASTM standard. The specimens were cast against a polymeric half-cylinder substrate with the same dimensions, demoulded after one day and stored for 28 d in a moist room at 95 % ± 5 % RH and 20 °C ± 2 °C; all reported uncertainties represent one standard deviation, unless stated otherwise.

A total of five series were cast. The specimens were manually ground (bonded surface) by means of a sand paper until the desired roughness was reached. The International Concrete Repair Institute (ICRI) has a set of "roughness" surface profile chips [19]. An intermediate profile, similar to the CSP-5 chip, was targeted at an age of 28 d. All prepared surfaces were visually similar. Three out of five surfaces were used for the bacterial treatment (BAC, BACX and BAC#, see later on). One series was used for reference samples (REF). One series of three specimens were not manually ground and the casting surface was used in further testing. These smooth specimens served to study the influence of the roughness (SMO).

2.2 Bacterial strain and cultivation condition

Bacillus sphaericus LMG 22257 (Belgian coordinated collection of microorganisms, Ghent) was used in this study. The bacteria were grown aseptically in the growth medium (400 mL per batch) that consisted of a blend of yeast extract (20 g/L) and urea (20 g/L). The culture was incubated at 28 °C on a shaker at 10.5 rad/s [100 rpm] for 24 h. Subsequently, the bacterial cells were harvested by centrifugation (733.0 rad/s [7000 rpm], 7 min) of the 24 h old grown culture and were re-suspended in sterile saline solution (NaCl, 8.5 g/L). The concentration of the bacteria in the suspension typically varied from $1.5 \cdot 10^9$ cells/mL to $2 \cdot 10^9$ cells/mL. The obtained bacterial suspension was stored in a 4 °C refrigerator for further experimental use.

2.3 Biodeposition treatment

Three different biodeposition patterns were studied. These include a continuous layer, a non-continuous layer with two thirds of the surface covered by biodeposition and a non-continuous layer with only one third of the surface covered by biodeposition. For this purpose, the mortar substrate surfaces were taped with aluminium tape in a distinct way (Figure 1). In an eventual biodeposition, a film would be deposited both on the mortar surface and the tape. By removing the tape after the biodeposition, only the uncovered parts of the mortar substrate would have been treated. In that way, the three different series with 100% biodeposition (BAC), 66% biodeposition (BACX) and 33% biodeposition (BAC#) were made.

Mortar specimens (BAC, taped BACX and taped BAC#) were partially immersed in a precipitation medium that consisted of urea (0.5 mol/L), calcium nitrate (0.5 mol/L) and yeast extract (5 g/L) for 24 h. The medium level was approximately 10 mm above the immersed surface (elliptical surface for applying repair material) of the mortar specimens. After that, the specimens were taken out from the precipitation medium and put upside down until surface dry at 60 % ± 5 % RH and 20 °C ± 2 °C. Subsequently, bacterial suspension was sprayed (approximately 0.5 mL/cm²) all over each elliptical surface every 6 h for 4 times. In the end, the biodeposition layer was seen on all samples (Figure 2). After 3 days, the repair mortar was applied.

2.4 Repair material application and slant shear testing at 28 d

The repair material (Sika MonoTop-412 N)[1] was mixed for 3 min. It is a cement-based single component fiber reinforced repair mortar with low shrinkage and with R4 classification according to EN 1504-3. The prepared bonding surface (mortar half cylinder) was put inside of a cylindrical mould (as replacement of the polymeric half-cylinder substrate) and the repair material was applied next, filling the cylindrical mould. The complete specimen was demoulded the day after. The entire cylinder was put in a moist room at 95 % ± 5 % RH and 20 °C ± 2 °C until the repair product achieved an age of 28 d. Prior to testing, the loading surfaces of each cylinder were ground to produce a smooth and parallel testing surfaces. The composite specimen was loaded in compression (Figure 3) and its strength was recorded, as described in the Standard ASTM C882/C882M − 13. The bond strength was determined by dividing the load carried by the specimen at failure by the area of the bonded surface. The area of the bonded surface was reduced by that of any visible voids found in the bond layer on inspection after the test. Specifically, only voids larger than 3 mm in diameter were considered, as mentioned in the Standard ASTM C882/C882M − 13. Almost no big voids were observed.

[1] Certain commercial products are identified in this paper to specify the materials used and the procedures employed. In no case does such identification imply endorsement or recommendation by Ghent University or the National Institute of Standards and Technology, nor does it indicate that the products are necessarily the best available for the purpose.

2.5 Characterization of the interface between mortar substrate and repair material

The mineral phases in the mortar-biodeposition layer-repair material interface were investigated by use of X-ray diffraction (XRD), Scanning Electron Microscopy (SEM) and thin section analysis. After the slant shear test, shards from the mortar surface, repair material surface and biodeposition layer were carefully and manually collected using a spatula.

A copper X-ray tube was used for the XRD analysis with Cu K(alpha) radiation at 40 kV and 40 mA and a wavelength of 0.154 nm. The samples were manually trimmed into about 1 cm in diameter and 2 mm to 3 mm thick pieces to fit the sample holder. Scanning was performed from 10° to 70° two-theta with a step size of 0.039°. The different compositions on the surfaces were studied and determined.

Samples for SEM analysis were first subjected to a gold coating process to ensure good electrical conductivity. SEM analysis was performed on an instrument operating at an acceleration voltage of 20 kV and equipped with an Energy-Dispersive X-ray analyzer (EDX detector). In that way, the crystals present could be examined for their composition. The mortar substrate surface, biodeposition layer and the surface of the repair mortar after slant shear testing were studied.

To study the crystals formed at the interface between the mortar substrate and the repair material, thin sections (40 mm × 25 mm × 25 μm) were prepared from the slant shear specimens, perpendicular to the interface and along the height of the cylindrical specimen (Figure 3). First, the specimens were cut to expose 40 mm × 25 mm faces that were then mounted on a glass slide with a thickness of 2.9 mm. The combined sample was cut and polished until a height of the specimen and glass of 10.1 mm was reached. Next, the specimens were impregnated under vacuum with a fluorescent epoxy. The excess epoxy was polished away and an object glass was glued on the smooth surface. Finally, the glass slides were cut off and the remaining part was polished until a thin section with 25 µm thickness was achieved. A cover glass was glued on top to protect the thin section. The thin sections were then analysed under normal and fluorescent light [20].

3. Results and discussion

3.1 Study of the biodeposition layer

The complete system for the bacterially treated specimens is shown in Figure 4. A clear whitish layer can be seen located in between the mortar substrate and the repair material. The white colour and high birefringence under visual and normal light gives the hint that this may be calcium carbonate ($CaCO_3$), as will be studied later on by means of EDX. No corresponding white layer can be found in the reference specimens. The whitish layer appeared to adhere well to the mortar substrate and showed a rough texture towards the repair material surface. This surface, together with the formed polymorphs (as studied later on), will be responsible for a possible increase in bond. The $CaCO_3$ layer in the bacterial specimens has an average thickness of 52 µm ± 14 µm (n = 250). This thickness is consistent with thicknesses of bacterial depositions found in literature [11, 16].

The layer can be further engineered depending on the method of application. Here, a bacterial suspension was sprayed four times to ensure the overall thickness of the bacterial layer. This method can be altered to receive the optimal layer for a specific condition. Here, it was decided to study an approximately 50 µm thick layer to improve the bond strength of the repair material on the mortar substrate.

3.2 Slant shear strength tests

The results obtained when performing a compression test on the slant shear specimens, are shown in Table 1 and Figure 5. The elliptical surface area was measured after the test. Possible defects at the edges and larger air voids were subtracted from the measured area. These parts did not take part in shearing and thus needed to be subtracted from the overall elliptical surface. The amount of such defects and larger air voids was not substantial and a homogeneous testing surface was obtained for all tested specimens. There were no artifacts while loading and the failure mechanisms of the composite cylinders were typical ones. The crack plane went through the interface. No brittle failure at the testing surfaces or possible crushing of the mortar was observed. A typical shear-type of failure was observed in all series tested.

Studying the effect of the roughness, it is found that a rougher surface leads to higher slant shear strengths. The reference sample (REF), with a CSP-5 roughness, has a 36 % higher shear strength compared to the smooth sample (SMO) with the original casting surface. This result was to be expected and has been found by other researchers as well [8, 21, 22]. Even lower values for the bond strength on cast concrete substrates have been found [23]. This is mainly dependent on the mixture studied, the setup, as well as the sample preparation. The reference surfaces, manually sand-paper ground, are comparable to the rougher surfaces commonly found in the literature. These showed higher slant shear strength. This is due to the fact that there will be a mechanical interlock contribution from the uneven surface texture leading to an increase in the nominal bond strength as the shear resistance is increased.

When comparing the results obtained with the bacterially treated specimens, it is found that the slant shear strength increases even further. The strength is 10 %; 16 % and 50 % higher compared to the REF sample for BAC, BACX and BAC#, respectively. Only the difference with BAC# is significant. The bacterial treatment thus seems to improve the overall bonding strength of the repair material to the mortar substrate. Again, there will be a mechanical interlock increasing the bond strength. In Figure 4, a rough surface may be co-responsible for the higher value of the slant shear strength found in the BAC specimens. Furthermore, the applied bacterial pattern layer caused an additional step-wise alteration of the surface where the approximately 50-µm thick bacterial layers are interrupted by plain mortar substrate surfaces. This increased the mechanical interlocking even further, leading to the higher values of slant shear strength found.

In preliminary experiments performed on analogous materials [24], a biodeposition layer was applied on two mortar substrates and a 2-mm layer of repair mortar was applied in between. The same slant shear test was conducted and it was found that the average results for the slant shear strength of the bacterially treated specimens were 13 % higher compared to the un-treated specimens. The results were not statistically different from each other. Here, the bacterial interface zone contributed twice and the failure mechanism was a combination of shear failure along the interface and through the repair mortar layer. As the layer was quite thin, no significant differences were found, but there was a suggestion that the bacterial layer increased the bond to some extent.

Figure 6 shows the elliptical surface of one specimen per series after performing the slant shear test. The surfaces of the smooth and reference samples are clean and debonding of the repair material layer from the mortar surface occurred. Conversely, a clear whitish layer was observed on the bacterially treated specimens and was still observable after testing the specimens. This resulted from the calcium carbonate biodeposition due to the bacterial treatment, as mentioned previously. Partial debonding of the calcite layer deposited by the bacteria is seen by comparing the bonding surfaces after the compression test of the composite cylinder (Figure 6). Some biodeposition adhered to the repair mortar. The found rougher surface is thus possibly primarily responsible for the increase in slant shear bond strength. A combination of both the mortar surface and the biodeposition interface can be seen for the partially bio-treated specimens where a biodeposition pattern was applied. The grey mortar is interrupted by diamond-shaped biodeposition. The further increase in slant shear strength is possibly due to the stepwise formation of the calcium carbonate layers due to the use of the aluminium tape. This may cause a higher mechanical interlocking through the shear plane during slant shear testing.

3.3 XRD and SEM analysis of the carbonates

The XRD spectra are shown in Figure 7 and the SEM images and EDX spectra in Figures 8-10. These were used to study the polymorphic forms of the biodeposition. The type of polymorph can have an effect on the bonding of new hydrates on the surface [25].

The biodeposition film on the mortar surface mostly consisted of calcite and vaterite (Figure 7). Diffraction patterns show strong patterns corresponding to calcite and vaterite, both polymorphs of $CaCO_3$ (green curve). The compositions of the mortar substrate and repair material surfaces were quite similar, as they are both cementitious materials. They both contained calcite, vaterite and quartz. The detailed percentage of each mineral is unknown from this qualitative analysis. Yet it can be seen that calcite was the main mineral, while the amount of vaterite appears to be lower than that of calcite on the mortar substrate and repair material surfaces. This can be judged by the fact that the dominant diffraction peaks of vaterite were very weak in the spectra of the samples from mortar substrate and repair material surfaces (blue and red curve). No calcium hydroxide (CH) or calcium silicate hydrate (C-S-H) was found on the surfaces, suggesting that they were highly carbonated. Nor was aragonite, the third polymorph of $CaCO_3$, indicated in any of the XRD spectra.

Vaterite is typically the major product formed in the pH-range between 8.5 and 10. Conversely, aragonite preferably forms at pH 11, while calcite is the dominant product when the pH is higher than 12, at laboratory temperature [26]. Vaterite is a metastable polymorph of calcium carbonate and is rare in natural environments [27], transforming to calcite (or aragonite) at room temperature in an aqueous solution [28]. However, vaterite can be synthesized in chemical processes and often forms in the presence of microorganisms [29]. This gives an indication that bacteria and their secretions (mainly organic compounds) may facilitate the formation of vaterite.

The three kinds of surfaces had completely different distinct morphologies. Some foil-like structures, originating from CSH can be seen on the mortar surface in Figure 8c. While on the repair material, surface particles of a size ranging from 2 µm to 5 µm can be seen (Figure 9c). Based on the EDX spectrum, these particles might be Ca-Mg-carbonates, originating from the specific composition of the repair material. The biodeposition film was full of bacterial imprints (Figure 10d). These imprints can be seen as long elliptical shaped spots with a length of approximately 2 µm. The EDX spectra indicated that the film was mainly composed of calcium carbonate. The film was not flat; instead, it was rough with a lot of pits. This could be due to roughening of the mortar surface with sand paper and due to the irregularly formed calcium carbonate crystals.

The formed polymorphs, together with the rougher surface, are responsible for the increase in the bond strength. On one hand the bond on calcite and vaterite, as found in the biodeposition layer of the repair material, could be higher. Fine micrometer-sized particles of calcite are known to accelerate cement hydration and in general, cement paste (mortar) bonding to limestone coarse aggregates is superior to that found with siliceous aggregates [25]. On the other hand, the mechanical interlocking also seems to play a substantial role in the overall improvement of the bond strength in this present system.

3.4 Thin-section analysis

Thin-section analysis is useful in effectively investigating the interlayer between the mortar substrate and the repair material in case of the reference samples and the interlayer between the mortar, calcium carbonate (biodeposition) layer and the repair material, respectively, for the bacterially treated specimens (Figure 11). In the case of the reference sample, the crack (yellow-green region) propagated through the interface of the mortar substrate and the repair material. A clean and smooth cracking pattern along the interface is found. This seems to be the weakest link when applying the repair material on the mortar surface with only a manual roughening procedure using sandpaper, as was the case for this research. That is why this biodeposition layer seems to be a promising avenue to increase the overall bond between the mortar substrate and the repair material.

The formed $CaCO_3$ layer has a rough surface due to the formation of irregular crystals (Figure 4 and Figure 11). Both the repair material and the mortar substrate tend to show a good adherence to that layer. This roughness could also partially lead to the increase in observed bond strength. In the case of the bacterial treated specimens, it could be seen that debonding takes place in the repair material near the vicinity of the $CaCO_3$ layer or in the interface between the layer and the substrate. Both the bonding with the mortar substrate and the repair material seems to be sufficient to increase the bond strength. Furthermore, locations are noted where the crack was found in the repair material further away from the interface (no debonding in Figure 11). This shows the beneficial effect that the biodeposition layer has in terms of the slant-shear strength increase.

4. Conclusions

Based on this initial study of applying a biodeposition layer for bond enhancement of repair materials, the following conclusions can be drawn:

- A bacterial treatment has been shown to enhance the bonding of a repair product to a mortar substrate.
- Even higher bonding properties are obtained when using an irregular layer of biodeposition. This engineered pattern layer seems to be a promising route to increasing the bond of a repair material to a mortar substrate, mainly due to the influence of increased mechanical interlocking.
- The biodeposition film on the mortar surface mostly consisted of calcite and vaterite, possibly increasing the bond of products formed by the repair material on the mortar substrate.
- Both the mortar substrate and the repair material exhibited a good bonding with the calcium carbonate crystals precipitated by the bacteria.
- The formed vaterite and calcite polymorphs, together with the rougher surface, are responsible for the increase in the bond strength. This shows the potential of the biodeposition application for increasing the bond between the mortar substrate and the repair material and thus also the slant shear strength of the overall composite.

Acknowledgements

As Postdoctoral Research Assistants of the Research Foundation-Flanders (FWO-Vlaanderen), Didier Snoeck and Jianyun Wang would like to thank the foundation for its financial support.

Certain commercial products are identified in this paper to specify the materials used and the procedures employed. In no case does such identification imply endorsement or recommendation by Ghent University or the National Institute of Standards and Technology, nor does it indicate that the products are necessarily the best available for the purpose.

References

[1] D. Snoeck, N. De Belie, From straw in bricks to modern use of microfibres in cementitious composites for improved autogenous healing – a review, Constr Build Mater, 95 (2015) 774-787.

[2] K. Van Tittelboom, N. De Belie, Self-Healing in Cementitious Materials - A Review, Materials, 6 (2013) 2182-2217.

[3] J. Wang, D. Snoeck, S. Van Vlierberghe, W. Verstraete, N. De Belie, Application of hydrogel encapsulated carbonate precipitating bacteria for approaching a realistic self-healing in concrete, Constr Build Mater, 68 (2014) 110-119.

[4] G.P. Tilly, J. J., Concrete repairs, Performance in service and current practice, in, CONREPNET, 2007.

[5] K. Minoru, K. Toshiro, U. Yuichi, R. Keitetsu, Evaluation of bond properties in concrete repair materials, J Mater Civ Eng, 13 (2001) 98-105.

[6] G. Xiong, J. Liu, G. Li, H. Xie, A way for improving interfacial transition zon between concrete substrate and repair materials, Cem Concr Res, 32 (2002) 1877-1881.

[7] G. Xiong, B. Luo, X. Wu, G. Li, L. Chen, Influence of silane coupling agent on quality of interfacial transition zone between concrete substrate and repair materials, Cem Concr Comp, 28 (2006) 97-101.

[8] S. Austin, P. Robins, Y. Pan, Shear bond testing of concrete repairs, Cem Concr Res, 29 (1999) 1067-1076.

[9] B. Bissonnette, L. Courard, A. Garbacz, A.M. Vaysburd, K.F. von Fay, Development of Specifications and Performance Criteria for Surface Preparation Based on Issues Related to Bond Strength, in: U.S.D.o.t. Interior (Ed.), U.S. Department of the Interior, 2017.

[10] B. Bissonnette, A.M. Vaysburd, K.F. von Fay, Best Practices for Preparing Concrete Surfaces Prior to Repairs and Overlays, in: U.S.D.o.t. Interior (Ed.), U.S. Department of the Interior, 2012, pp. 92 pp.

[11] W. De Muynck, N. De Belie, W. Verstraete, Microbial carbonate precipitation in construction materials: A review, Ecological Engineering, 36 (2010) 118-136.

[12] J.P. Adolphe, J.F. Loubière, J. Paradas, F. Soleilhavoup, Procédé de treitement biologique d'une surface artificielle, in: E. patent (Ed.), Europe, 1990.

[13] G. Le Metayer-Levrel, S. Castanier, G. Orial, J.F. Loubiere, J.P. Perthuisot, Applications of bacterial carbonatogenesis to the protection and regeneration of limestones in buildings and historic patrimony, Sedimentary Geology, 126 (1999) 25-34.

[14] C. Rodriguez-Navarro, M. Rodriguez-Gallego, K. Ben Chekroun, M.T. Gonzalez-Munoz, Conservation of ornamental stone by Myxococcus xanthus-induced carbonate biomineralization, Appl Environ Microbiol, 69 (2003) 2182-2193.

[15] W. De Muynck, S. Leuridan, D. Van Loo, K. Verbeken, V. Cnudde, N. De Belie, W. Verstraete, Influence of pore structure on the effectiveness of a biogenic carbonate surface treatment for limestone conservation, Appl Environ Microbiol, 77 (2011) 6808-6820.

[16] W. De Muynck, K. Cox, N. De Belie, W. Verstraete, Bacterial carbonate precipitation as an alternative surface treatment, Constr Build Mater, 22 (2008) 875-885.

[17] W. De Muynck, D. Debrouwer, N. De Belie, W. Verstraete, Bacterial carbonate precipitation improves the durability of cementitious materials, Cem Concr Res, 38 (2008) 1005-1014.

[18] A. Momayez, M.R. Ehsani, A.A. Ramezanianpour, H. Rajaie, Comparison of methods for evaluating bond strength between concrete substrate and repair materials, Cem Concr Res, 35 (2005) 748-757.

[19] ICRI, Selecting and Specifying Concrete Surface Preparation for Sealers, Coatings, Polymer Overlays, and Concrete Repair with CSP Chips, in, ICRI, 2013, pp. 48.

[20] D. Snoeck, N. De Belie, Repeated autogenous healing in strain-hardening cementitious composites by using superabsorbent polymers, J Mater Civ Eng, 04015086 (2015) 1-11.

[21] L. Courard, T. Piotrowski, A. Garbacz, Near-to-surface properties affecting bond strength in concrete repair, Cem Concr Comp, 46 (2014) 73-80.

[22] L. Courard, A. Garbacz, Surfology: what does it mean for polymer concrete composites?, Restoration of Buildings and Monuments, 16 (2010) 291-302.

[23] P.M.D. Santos, E.N.B.S. Júlio, V.D. Silva, Correlation between concrete-to-concrete bond strength and the roughness of the substrate surface, Constr Build Mater, 21 (2007) 1688-1695.

[24] D. Snoeck, J. Wang, D.P. Bentz, N. De Belie, Bond enhancement of repair mortar via biodeposition, in: International conference on advances in construction materials and systems, ICACMS 2017, Chennai, 2017, pp. accepted.

[25] D.P. Bentz, A. Ardani, T. Barrett, S.Z. Jones, D. Lootens, M.A. Peltz, T. Sato, P.E. Stutzman, J. Tanesi, J. Weiss, Multi-scale investigation of the performance of limestone in concrete, Constr Build Mater, 75 (2015) 1-10.

[26] J. Watanabe, M. Akashi, Formation of various polymorphs of calcium carbonate on porous membrane by electrochemical approach, Journal of Crystal Growth, 311 (2009) 3697-3701.

[27] F. Lippmann, Sedimentary Carbonate Minerals, Springer, UK, 1973.

[28] N. Spanos, P.G. Koutsoukos, The transformation of vaterite to calcite: effect of the conditions of the solutions in contact with the mineral phase, Journal of Crystal Growth, 191 (1998) 783-790.

[29] S. Giralt, R. Julia, J. Klerkx, Microbial biscuits of vaterite in Lake Issyk-Kul (Republic of Kyrgyzstan), Journal of Sedimentary Research, 71 (2001) 430-435.

List of Tables

Table 1. Slant shear strength (n=3) of the studied samples with the average ($\bar{x}$) and the standard deviation (σ) for each case: SMO = smooth; REF = reference; BAC = bacterial sample; BACX = bacterial with 66% biodeposition; BAC# = bacterial with 33% biodeposition.

List of Figures

Figure 10. SEM images (a-d) and EDX spectrum of the red circle zone (e-f) of the biodeposition layer surface on the interface. The scale bar indicates 10µm. (e and f refer to the red circles in c and d, respectively)

Figure 11. Different forms of crack propagation in the reference samples (top) and the bacterially treated specimens (other). The scale bar indicates 125 µm.

Table 1. Slant shear strength (n=3) of the studied samples with the average ($\bar{x}$) and the standard deviation (σ) for each case: SMO = smooth; REF = reference; BAC = bacterial sample; BACX = bacterial with 66% biodeposition; BAC# = bacterial with 33% biodeposition.

	Slant shear strength [MPa]			
	#1	#2	#3	$\bar{x} \pm \sigma$
SMO	8.6	6.8	9.5	**8.3 ± 1.4**
REF	10.9	11.7	11.3	**11.3 ± 0.4**
BAC	11.8	13.0	12.6	**12.5 ± 0.6**
BACX	14.3	11.4	13.7	**13.2 ± 1.6**
BAC#	13.9	20.1	17.0	**17.0 ± 3.1**

BAC BACX BAC#

Figure 1. Biodeposition on the bacterial specimens showing the respective used tape pattern for partial deposition of 66% in BACX and 33% in BAC# specimens.

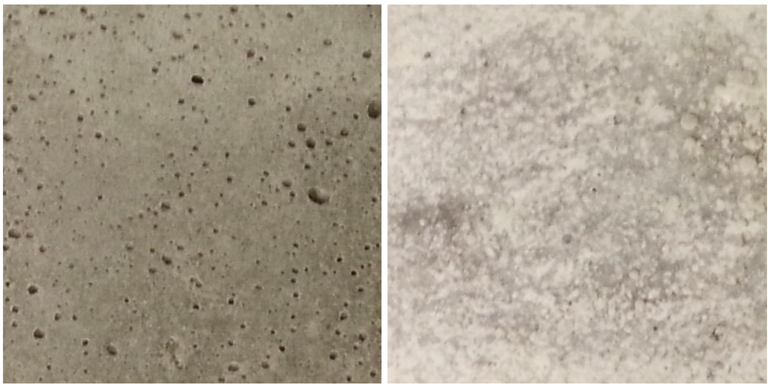

REF BAC

Figure 2. Appearance of the bonding surface of the substrate before (left) and after (right) bacterial deposition treatment.

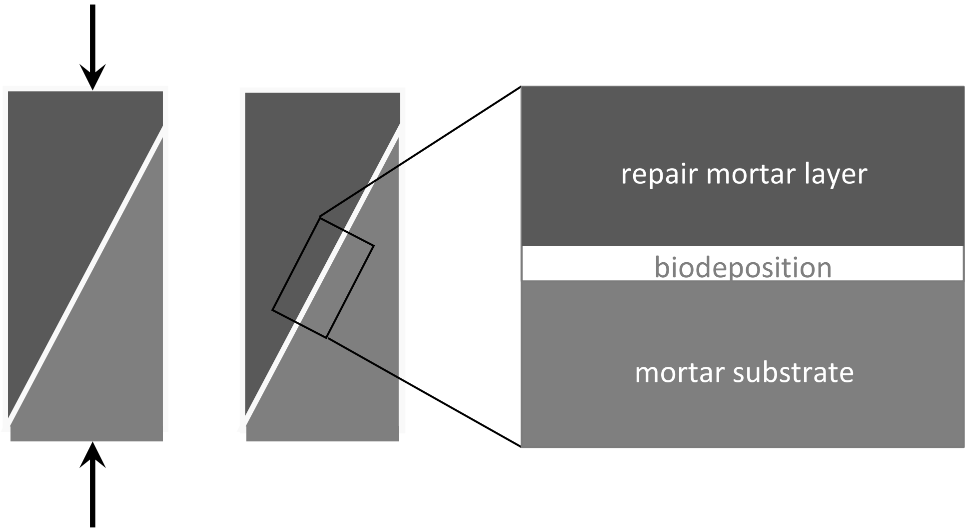

Figure 3. Slant shear setup showing the mortar substrate, biodeposition and repair material layer (left) and thin section location (right).

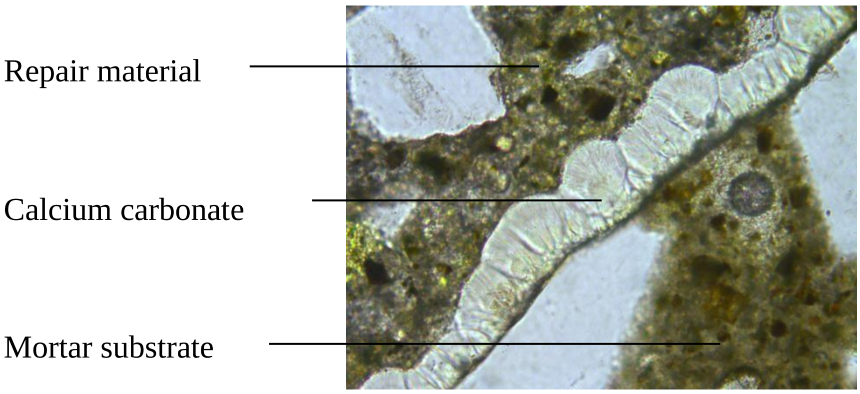

Figure 4. Micrograph with through-going plane-polarized light showing the formed biodeposition layer attributed to the bacterial activity at the interface between the mortar substrate and the repair material. The repair and mortar lines point to the hardened cement paste of each and the calcium carbonate line towards a single crystal. The figure width corresponds to 800 µm.

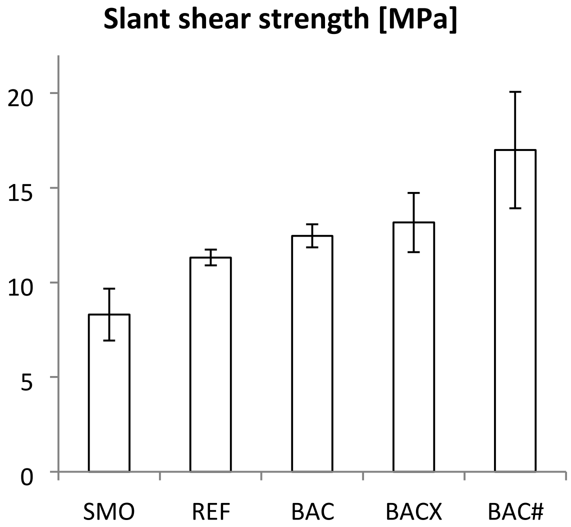

Figure 5. Slant shear strength results of the studied specimens showing the average (n=3) of all studied mixtures with the standard deviation on the single results.

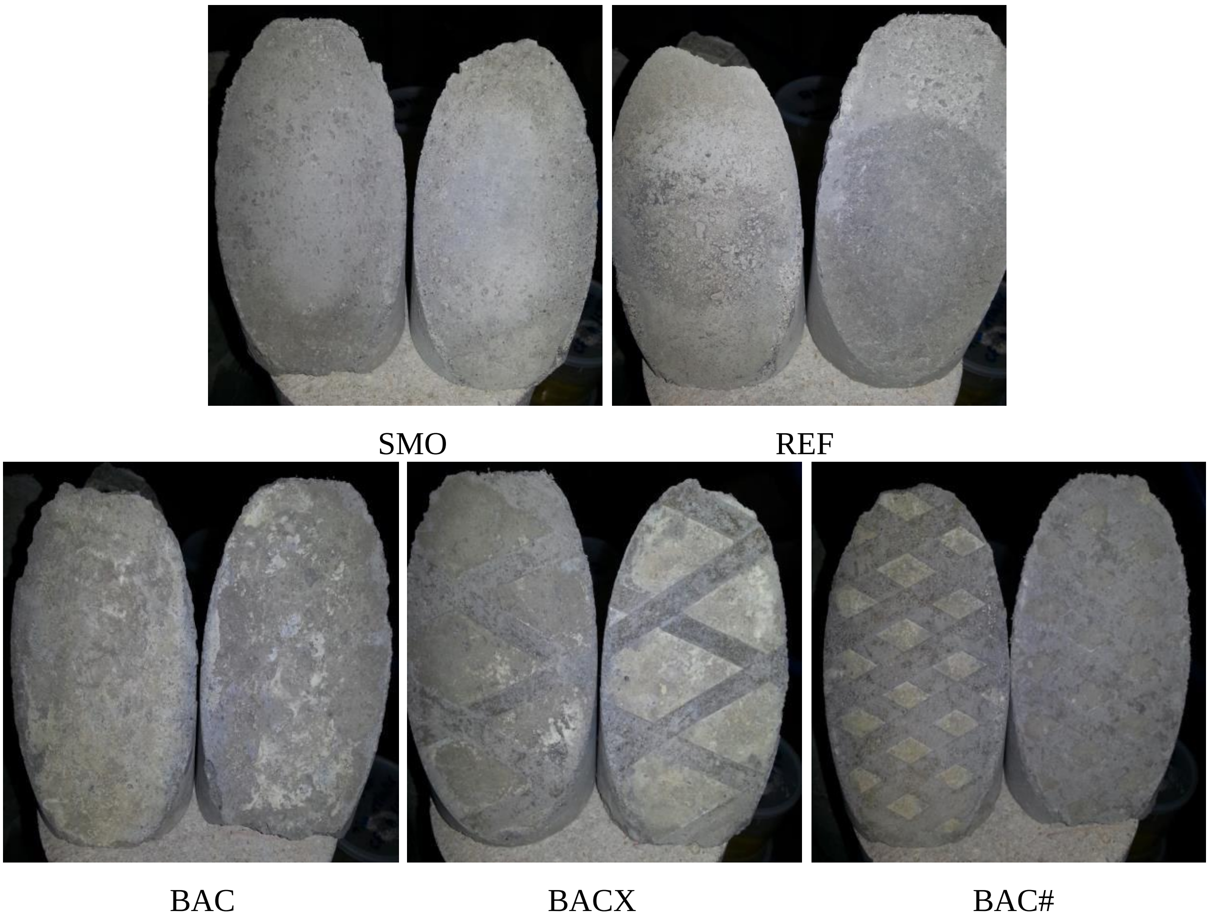

Figure 6. Elliptical interface surfaces after performing the slant shear tests of the studied specimens. (one representative example per treatment)

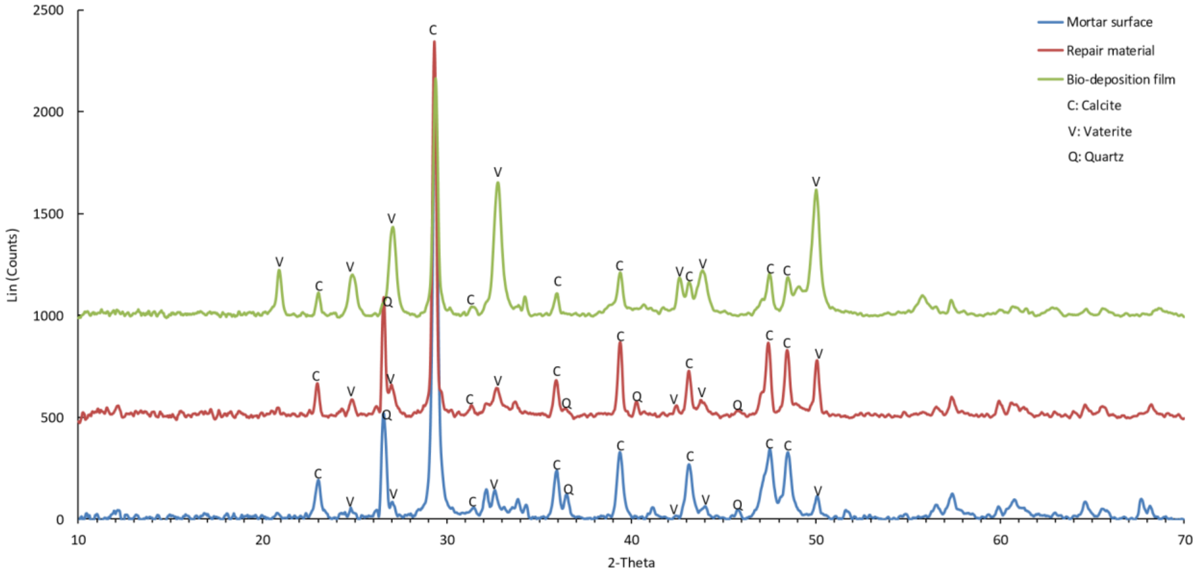

Figure 7. XRD spectra of the mortar substrate, repair material and the bio-deposition surface after slant shear testing.

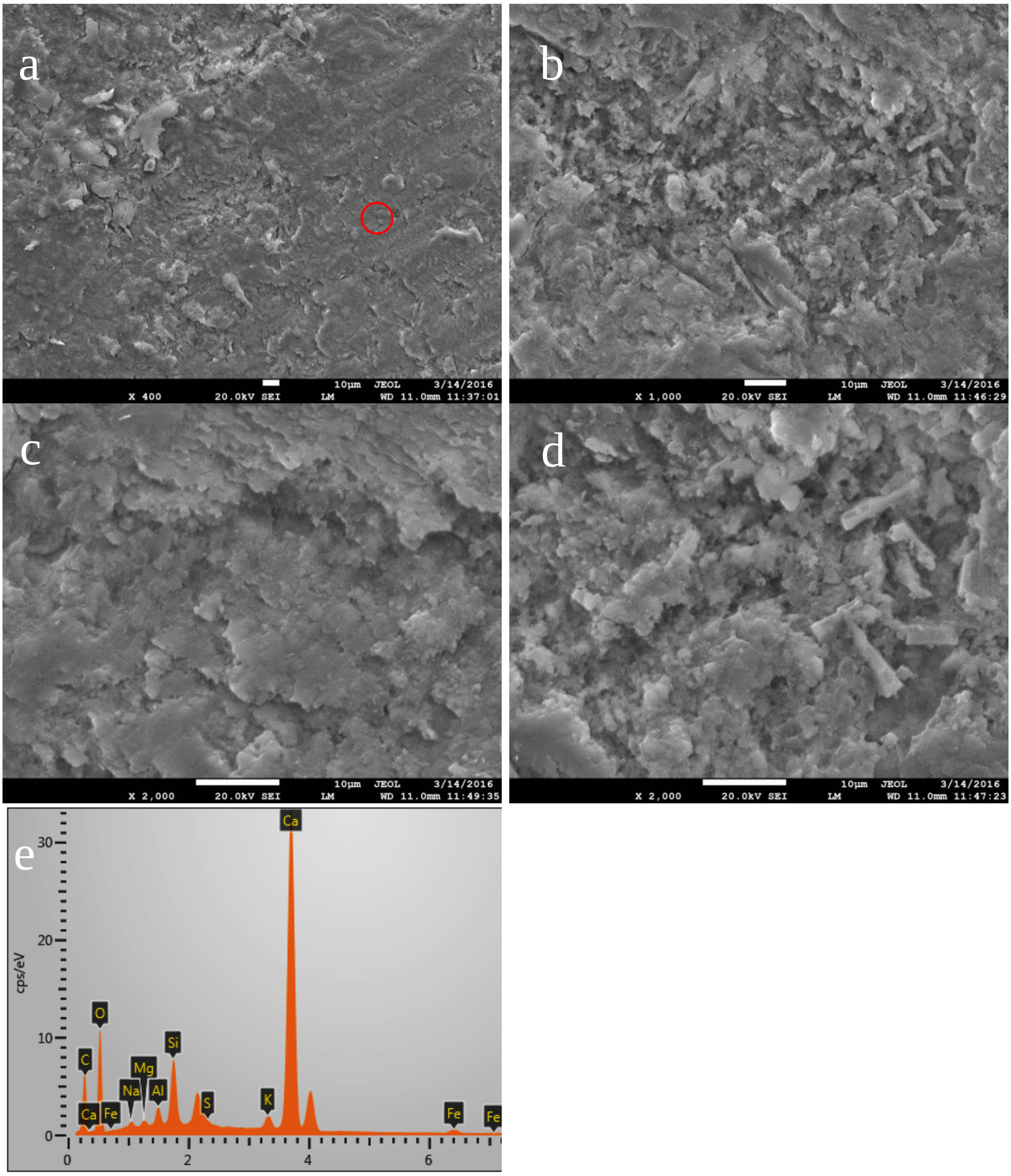

Figure 8. SEM images (a-d) and EDX spectrum of the red circle zone (e) of the mortar substrate surface. The scale bar indicates 10 µm.

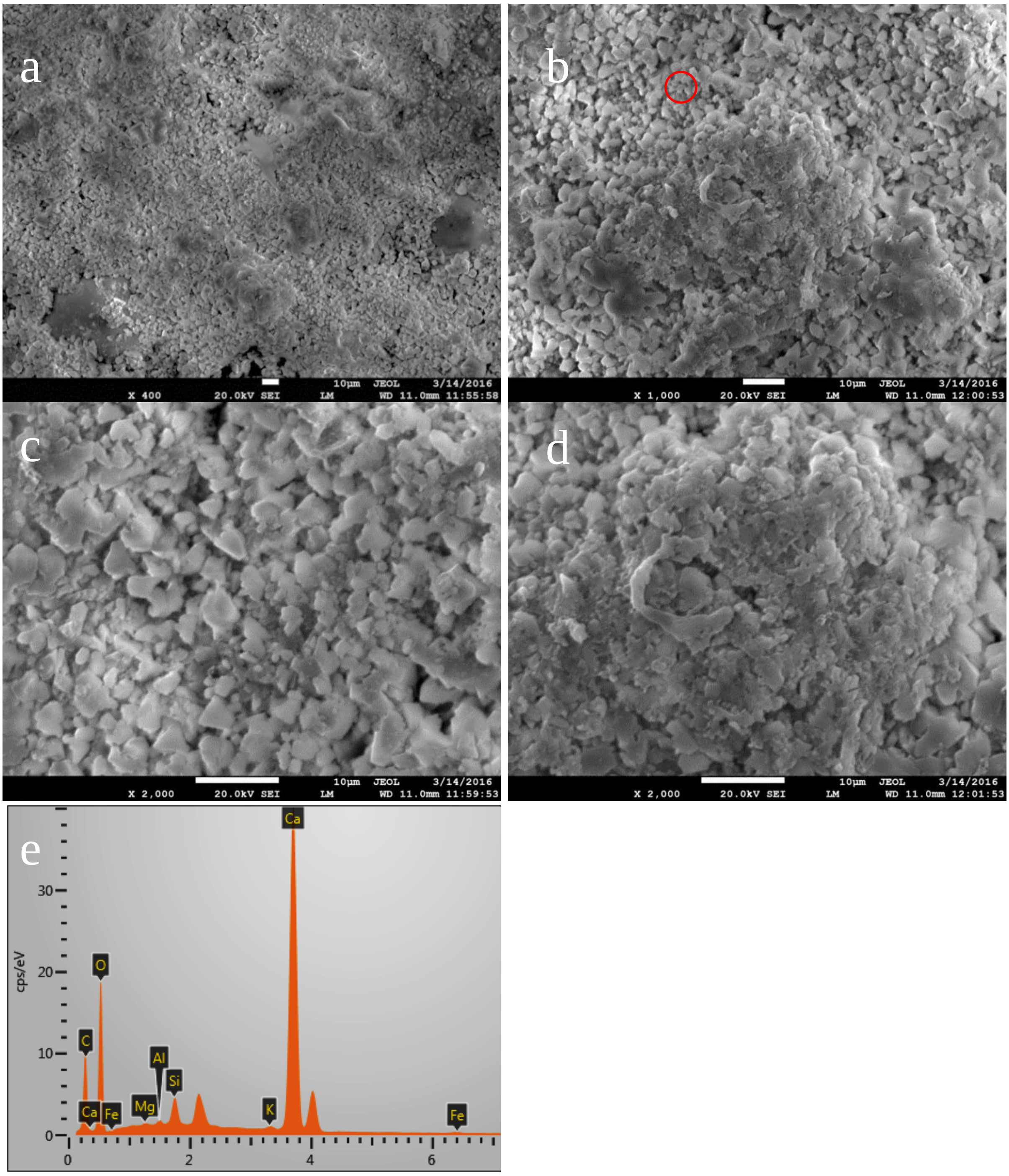

Figure 9. SEM images (a-d) and EDX spectrum of the red circle zone (e) of the repair material surface. The scale bar indicates 10 µm.

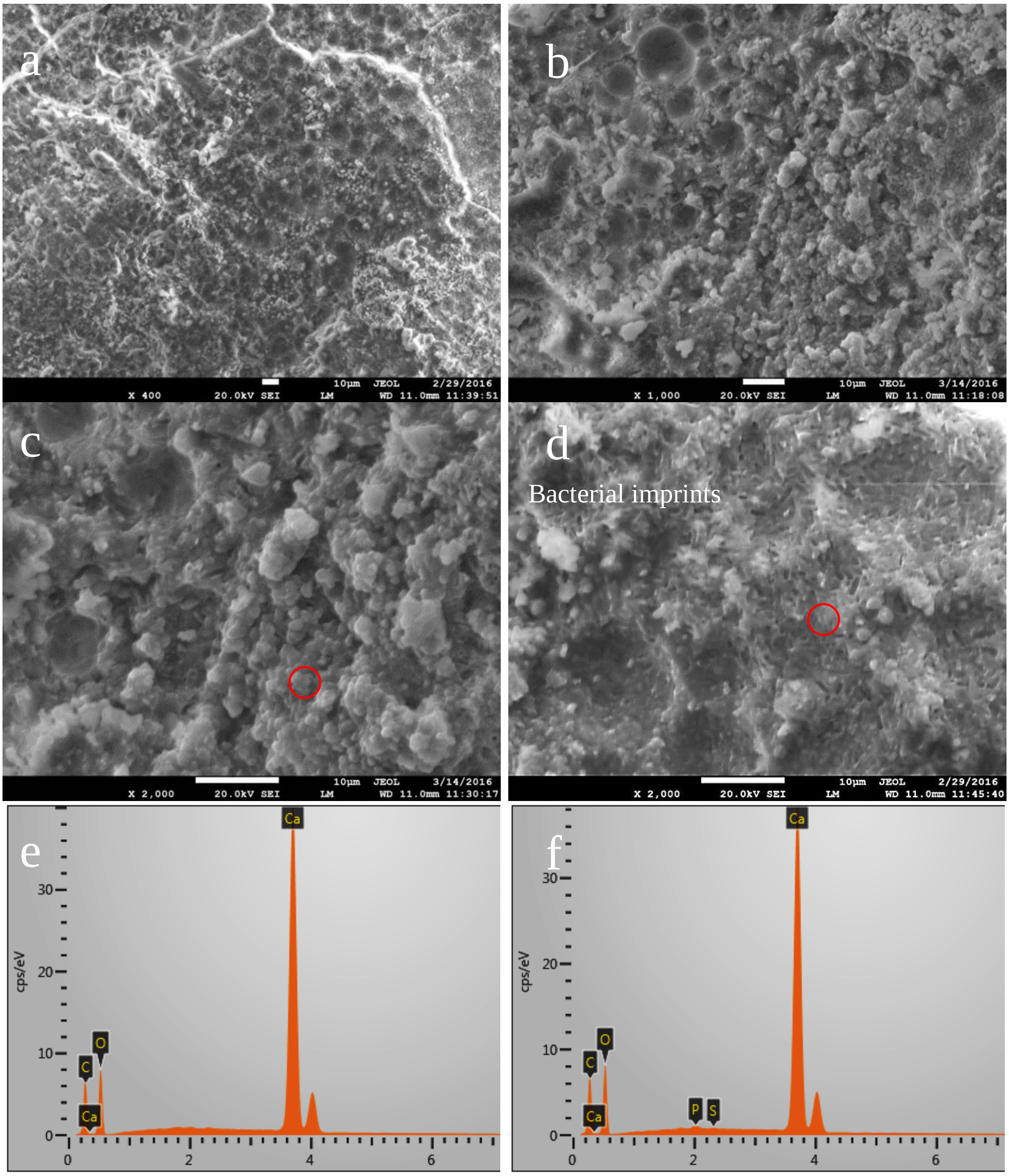

Figure 10. SEM images (a-d) and EDX spectrum of the red circle zone (e-f) of the biodeposition layer surface on the interface. The scale bar indicates 10 µm. (e and f refer to the red circles in c and d, respectively)

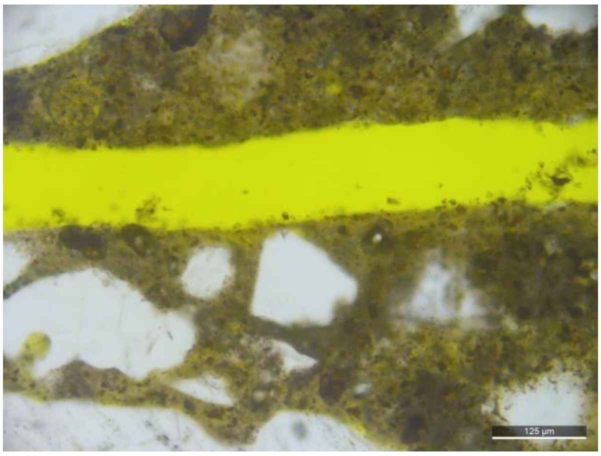

Clean shear failure in the reference mixture

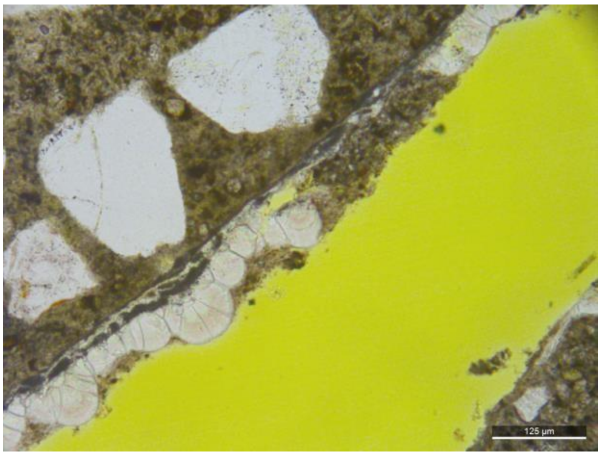

Crack near interface $CaCO_3$ and repair mortar

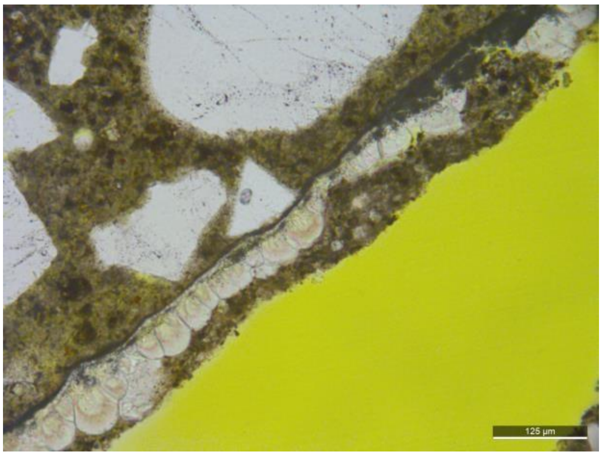

Crack in the repair mortar

Debonding of $CaCO_3$ near substrate

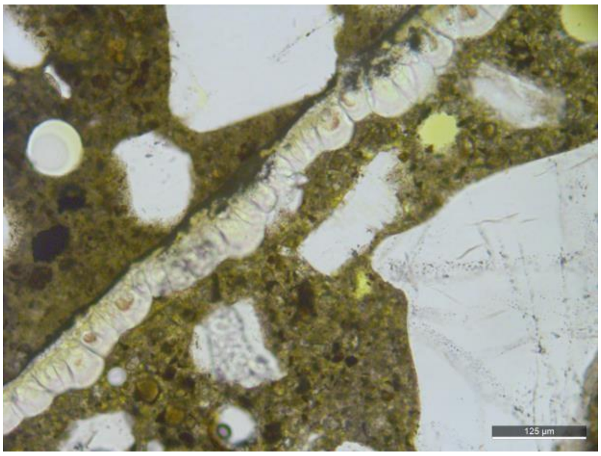

Slight debonding of $CaCO_3$ layer

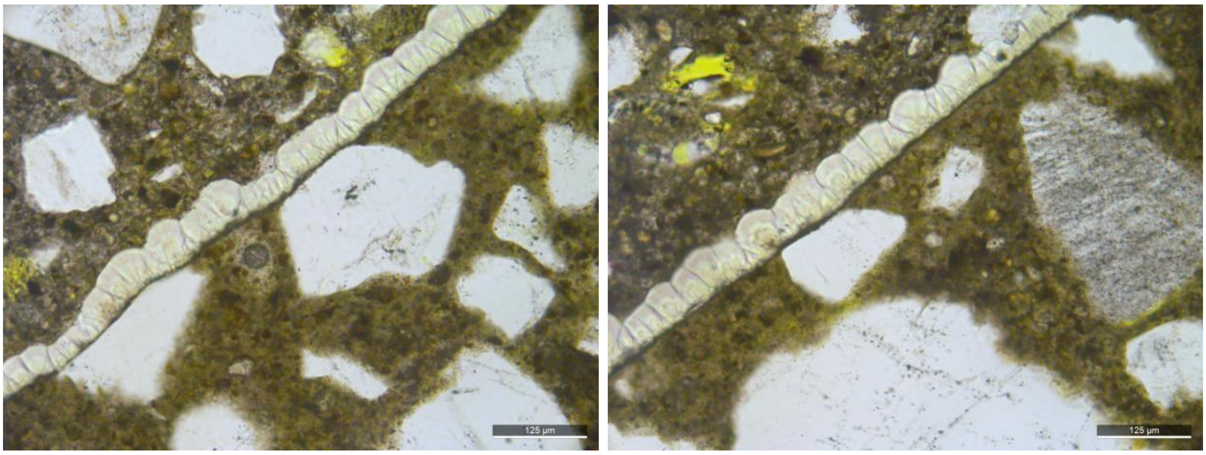

No debonding *No debonding*

Figure 11. Different forms of crack propagation in the reference samples (top) and the bacterially treated specimens (other). The scale bar indicates 125 µm.